

Practical approach to introducing potential-dependent chloride corrosion threshold in reinforcement corrosion predictive models

Andrea N. Sánchez
DNV GL
5777 Frantz Road
Dublin, OH 43017 U.S.A.

Alberto A. Sagüés
University of South Florida
Department of Civil and Environmental Engineering
4202 East Fowler Ave.
Tampa, FL 33620 U.S.A.

ABSTRACT

When passive steel is cathodically polarized by nearby previously corroding steel, the local value of chloride corrosion C_T could increase substantially, slowing down the spread of corrosion. The potential-dependent threshold (PDT) effect was introduced in an initiation-propagation mathematical model that simulated a partially submerged reinforced concrete column in sea water. Results indicated that when PDT is ignored, meaning a system with potential-independent threshold (PIT), the corrosion damage prediction can be overly conservative and may lead to structural overdesign. This issue is disregarded by present forecast models which assume only time invariant C_T values. Implementation of PDT is desirable but developing a mathematical model that forecasts the corrosion damage of an entire marine structure with a fully implemented PDT module may result in excessive computational complexity. This paper introduces an alternative, less computationally demanding module by incorporating PDT as an added feature to a traditional PIT forecasting model. A library of PDT and PIT paired cases were computed by changing the model input parameters over a wide range of values. Short-term and long-term corrosion damage outputs with PIT and PDT were statistically analyzed to identify a time-dependent, generic correction factor to adjust the corrosion damage functions estimated with the traditional PIT approach.

Key words: chloride corrosion threshold, steel, electric potential, corrosion, concrete, cathodic polarization, cathodic prevention

INTRODUCTION AND BACKGROUND

Corrosion of steel in concrete

Corrosion of steel in concrete is a major limitation to the durability of structures in marine service. The corrosion is principally attributable to the chloride ion penetration through the concrete cover. The chloride ions build up at the surface of the embedded steel until reaching a critical chloride threshold level (designated C_T) which causes breakdown of the protective passive film previously present at the steel surface due to the high alkalinity of the concrete. Passivity breakdown results in the onset of rapid

steel corrosion with accumulation of expansive corrosion products. The accumulation of corrosion products at the surface of the rebar results in an expansive force on the surrounding concrete causing tensile stresses to form in the concrete. As a result of the concrete's low tensile strength, the concrete subject to the previous conditions often cracks and spalls under those induced tensile stresses. Expensive maintenance repair and subsequent corrosion control is then necessary to extend the design service life. It is highly desirable to have accurate projections of the corrosion-related durability of structures either existing or under design to project future maintenance needs. The projections should be sophisticated enough to estimate not only the structure's age when substantial damage will appear but also the rate at which subsequent corrosion damage would develop.

Forecasting corrosion of steel in concrete

Durability models available at present calculate first the time for initiation of corrosion based on how rapidly the transport of chloride ions (often measured by an effective diffusion coefficient D) takes place through the concrete cover, thus establishing the amount of time needed to reach C_T (usually assumed to be time-invariant) at the steel position. A separate estimate is made for the time of propagation involving how long after the corrosion initiation will the expansive product accumulate enough to induce cracking or spalling in the concrete. The sum of both periods (time of initiation and time of propagation) yields the time to appearance of corrosion damage.¹ In any extended structure the concrete cover thickness X_C , diffusion coefficient D , surface chloride content C_S , and even the threshold C_T vary from point to point, and therefore damage appears earlier in some locations while in others the damage develops gradually. In a mathematical model, a statistical treatment based on the variability of the data can be used to predict the cumulative progression of that damage, called the "damage function" of the structure. An example of probabilistic corrosion damage projection based on the variability of X_C , D and C_S is shown in Ref. 2; comparable probabilistic approaches including also spatial variability of C_T and other variables are in common practice.³⁻¹⁰ Those models however tend to address C_T as a parameter that is independent of time, not affected by changes that may be taking place as the spatial corrosion pattern of the structure changes with time. Recent work has shown however that evolving corrosion profiles as a structure ages can significantly affect the local value of C_T and impact the damage projection accordingly.¹¹

Potential-Dependent Threshold (PDT)

The value of C_T is known to depend on several variables such as the condition of the steel surface and concrete properties, and, of special interest here, the potential of the steel while in the passive state.¹²⁻¹⁷ That dependence results in changes of C_T at the remaining regions of the steel assembly when some other regions reach the active condition as the structure ages, thus impacting the future corrosion development in a manner that is ignored if C_T is taken to be time invariant. The newly active regions develop more negative potentials than previously, so they tend to polarize the surrounding, steel passive regions in the cathodic direction. The resulting relative changes on C_T depend on the extent of macrocell coupling between active and passive steel assembly components.

Introducing Potential-Dependent Threshold in a forecasting model – Initial findings

To implement PDT in predictive models, it is first noted that a considerable amount of experimental evidence in the literature indicates that C_T increases as a result of cathodic polarization, following an exponential dependence in general of the form shown in Equation (1):¹⁴⁻¹⁷

$$\log_{10} \left(\frac{C_T}{C_{T0}} \right) \sim \frac{E_{T0} - E}{\beta_{C_T}} \quad (1)$$

where C_{T0} is the chloride threshold value at a baseline potential E_{T0} , E is the potential of the steel bar (while still in the passive condition), and β_{CT} (called the cathodic prevention slope), is the slope of the straight line corresponding to Equation (1) when plotted in an E - $\log C_T$ representation.¹¹ The redundant 3-parameter line formulation was chosen for convenience to match the form of other ruling equations in electrochemical systems.¹⁸ In the literature a wide range of β_{CT} values ranging from ~ 100 mV SCE to even ~ 700 mV have been suggested, but recent experimental work suggests that a value of 550 mV SCE¹/decade of chloride ion concentration may be prevalent, at least as a conservative bounding limit. That value has been adopted for the examples in this paper.^{11,15-17} It is noted in passing that the chloride threshold-changing effect is the basis of the cathodic prevention method, whereby reinforcing steel is cathodically polarized while still in the passive condition to delay or prevent corrosion due to the elevation of the chloride threshold.^{19,20}

An integrated corrosion initiation-propagation model that incorporated PDT for the case of a partially submerged reinforced concrete column in sea water was recently developed and demonstrated.⁴ Corrosion was assumed to start when C_T was reached in an active steel zone of a given size, followed by recalculating the potential distribution and update threshold values over the entire system at each time step. Notably, results of this work indicated that when PDT is ignored ($\beta_{CT} = \text{infinity}$) the corrosion damage prediction can be overly conservative which could lead to structural overdesign or misguided future damage management planning. A graphical representation is shown in Figure 1. The solid black line and the dashed line represent the results of the concrete surface damage function (DF) of a system with potential-independent threshold (PIT) and with PDT, respectively. To some extent the damage function progression for both cases during the first 25 years is similar, nevertheless, after that time period the corrosion DF for the PIT case is distinctly faster compare to the PDT. Clearly adequate implementation of PDT in next-generation models is important. This example illustrates how neglecting that feature could lead to an exceedingly conservative forecast, possibly adversely impacting decisions on how to allocate limited corrosion management resources in the future.

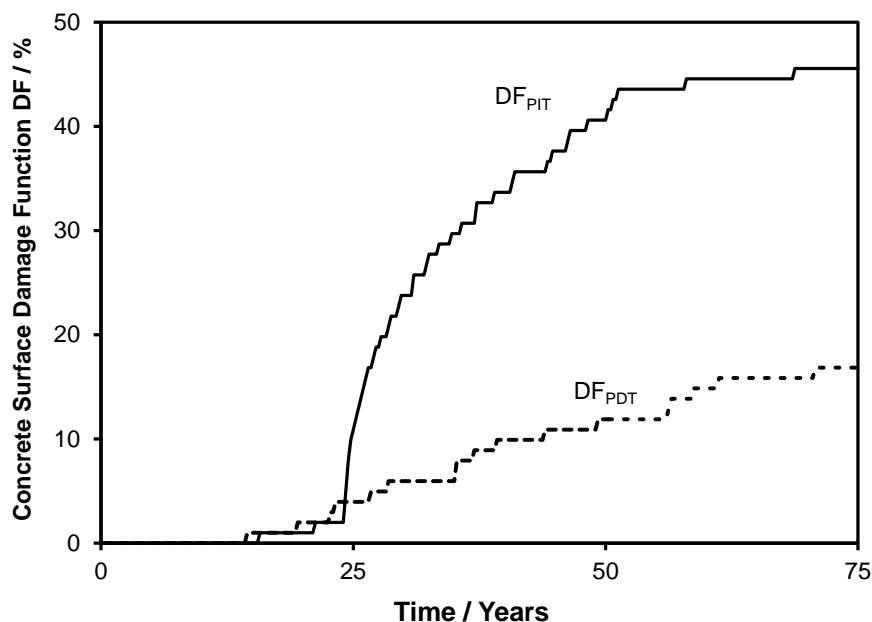


Figure 1: 75-year concrete surface damage function for the potential-independent (DF_{PIT}) and potential-dependent (DF_{PDT}) with β_{CT} of 550 mV.¹¹

¹ Saturated Calomel Electrode

Introducing Potential-Dependent Threshold in a forecasting model – Practical approach

Incorporation of PDT requires continuous updating of the corrosion distribution in a structure so that potential patterns are recalculated and local C_T values are adjusted accordingly. The intensive calculations used to demonstrate the PDT concept were conducted with a highly simplified system, to minimize computational demand¹¹. Those calculations were useful to develop insight on key factors of the problem, but extension of the approach to more realistic cases, for example to probabilistic models to forecast corrosion damage of an entire structure is a more daunting task. Detailed accounting for the variability of several parameters (e.g., X_C , D and C_S) with a fully implemented PDT module could create excessive computational complexity. This paper introduces an alternative, less computationally demanding means of incorporating PDT as an added feature to a traditional PIT forecasting model. The approach involves using a correction function to be applied to the projections that had already been computed using the PIT procedures. To that end, a library of PDT and PIT paired cases was computed using the previously mentioned simplified modeling approach, by changing the model input parameters over a wide range of representative values.^{14,15} The paired corrosion damage outputs with PIT and PDT were statistically analyzed to identify a time-dependent, generic γ correction factor to adjust the corrosion damage functions estimated with the traditional PIT method, and obtain an approximation of the corresponding PDT case output. The results are presented toward establishing a next-generation corrosion forecasting model for steel in concrete incorporating PDT features via this simplified approach.

MODELING

Cases examined

Two general schemes (Scheme 1 and Scheme 2) were examined for variation of exposure and concrete parameters with elevation, with focus on marine service structures and capture a variety of exposure and parameter modalities. The schemes were computed with a β_{CT} value of ~ 550 mV/decade of Cl^- concentration, based on the aforementioned experimental findings,^{11,15-17} and both schemes were also modelled with PIT ($\beta_{CT} = \infty$) pair cases.¹¹ Each of those schemes was implemented to obtain damage functions for low and high uniform concrete resistivity ρ situations (with consequently strong and weak macrocell coupling situations).

Scheme 1.

In Scheme 1, a reinforced concrete column partially submerged in seawater system was used with various elevation profiles of C_S , DO_2 and ρ that followed deterministic trends as those indicated in Figure 2, with parameters and variations (for DO_2 and ρ) listed in Table 1. The values of D and X_C were kept constant throughout the numerical simulation. These systems are generally based on the treatment described in Ref. 11, where each parameter is discussed in detail.

Scheme 2.

The system modelled in Scheme 2 is comparable to that simulated in Scheme 1 but only the atmospheric portion of the column was considered, as illustrated in Figure 3. Details for each parameter are given in detail elsewhere.²¹ The column ends were assumed to be electrically isolated and with a C_S of 0 kg/m². Random pattern profiles (as shown in Figure 3) were implemented for the chloride surface concentration C_S and the concrete cover X_C without the systematic overall trends that were assumed in Scheme 1. The C_S and X_C profiles were created using a random number generator and modified to minimize short wavelengths variations. Typical average values found in Florida marine structures, and somewhat exaggerated values of standard deviations to better reveal any possible effects from variability, were assigned to each profile and are listed in Table 2. Random variability was limited only to the values of C_S and X_C , two cases only one of each respectively parameter was assigned variability, and in another case class both varied simultaneously.

Table 1
Model parameters for the deterministic mathematical approach (Scheme 1)

Steel Cover	$X_C =$	7.5 cm		
Column diameter	$\Phi =$	105 cm		
Column Length	$L =$	1,200 cm		
Concrete Resistivity	$\rho_T =$	2×10^5 ohm-cm (Base); $\times 1/3, 1/10$ (Variations)		
	$\rho_S =$	4×10^4 ohm-cm (Base); $\times 1/3, 1/10$ (Variations)		
Oxygen diffusion coefficient	$DO_{2T} =$	10^{-3} cm ² /s		
	$DO_{2S} =$	10^{-5} cm ² /s		
		Log D varies linearly with elevation (Base) D varies linearly with elevation (Variation)		
Chloride diffusion coefficient	$D =$	2.5×10^{-8} cm ² /s		
O ₂ Surface Concentration	$C_{SO} =$	2.5×10^{-7} mol/cm ³ (in pore water)		
Cl ⁻ Surface Concentration	$C_{ST} =$	0 kg/m ³		
	$C_{SHT} =$	20 kg/m ³		
	$C_{SS} =$	9 kg/m ³		
Chloride Threshold Parameters	$C_{T0} =$	1.78 kg/m ³		
	$E_{T0} =$	-100 mV		
	$\beta_{CT} =$	550 mV/decade of Cl ⁻ (Base);		
Polarization Parameters**	E_0 (-mV SCE)		i_0 (A/cm ²)	Tafel Slope (mV)
	Iron Dissolution	-780	1.875×10^{-8}	60
Oxygen Reduction	160		6.25×10^{-10}	160
Steel Passive Current Density	$i_p =$	0.058×10^{-6} A/cm ²		
Critical Corrosion Penetration	$P_{CRIT} =$	0.01 cm		

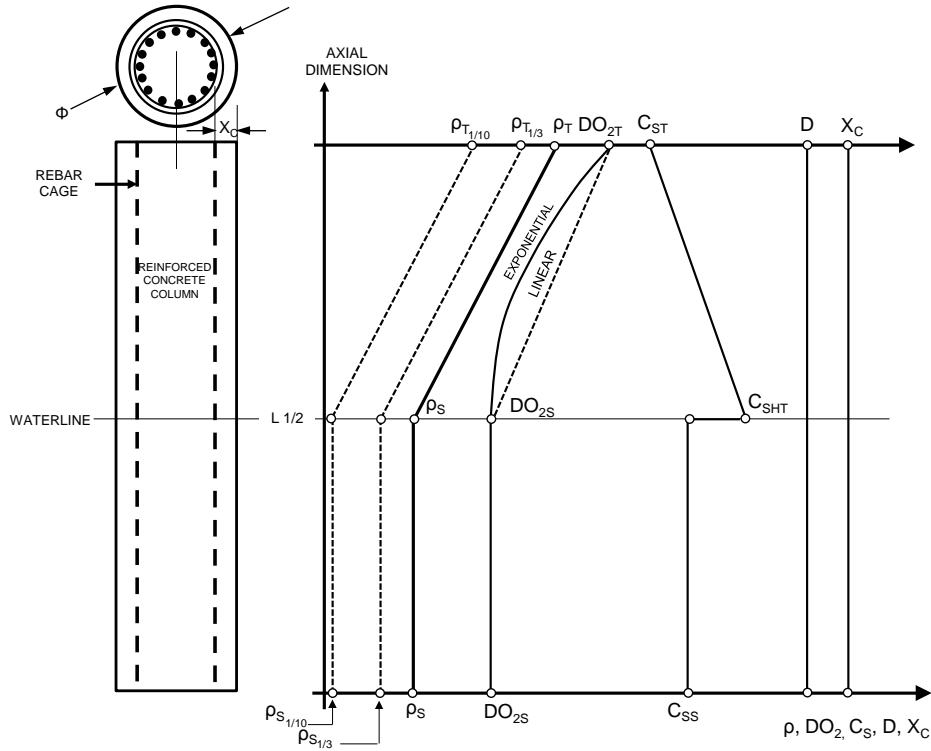


Figure 2: System modeled – Scheme 1: systematic variation of parameters.

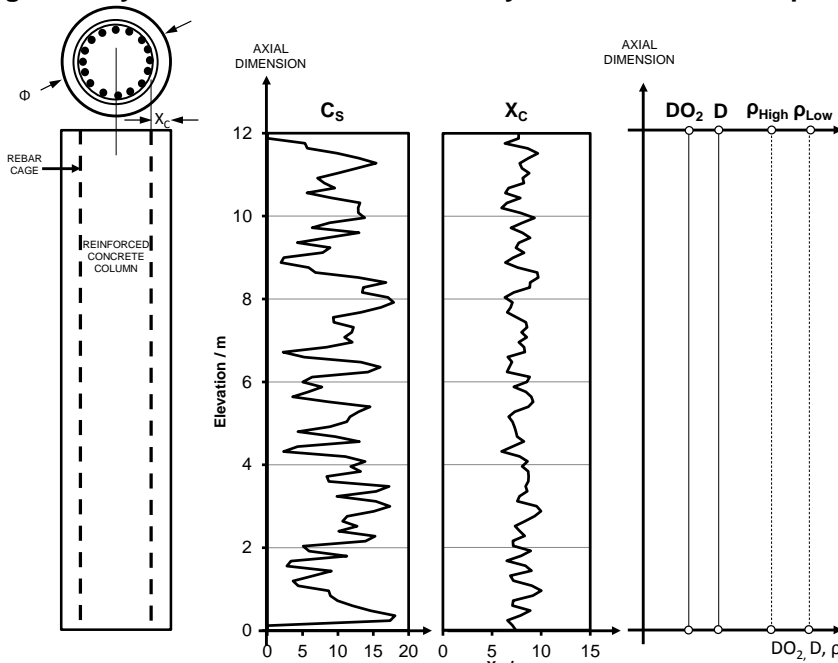


Figure 3: System modeled – Scheme 2: representative randomly distributed profiles for the surface concentration and concrete cover.

Table 2
Model parameters for the randomly distributed mathematical approach (Scheme 2)

Column diameter	$\Phi =$	105 cm		
Column Length	$L =$	1,200 cm		
Steel Cover (average)	$X_{Cavg} =$	8 cm		
Steel Cover (standard deviation)	$X_{Cstd} =$	2 cm		
Cl ⁻ Surface Conc. (average)	$C_{Savg} =$	10.4 kg/m ³		
Cl ⁻ Surface Conc.(standard deviation)	$C_{Sstd} =$	4.5 kg/m ³		
Concrete Resistivity	$\rho_{High} =$	7.5 × 10 ⁴ ohm-cm	(Base); ×1/3, 1/10	(Variations)
	$\rho_{Low} =$	1.5 × 10 ⁴ ohm-cm	(Base); ×1/3, 1/10	(Variations)
Oxygen diffusion coefficient	$DO_2 =$	2.5 × 10 ⁻⁵ cm ² /s		
Chloride diffusion coefficient	$D =$	2.5 × 10 ⁻⁸ cm ² /s		
O ₂ Surface Concentration	$C_{SO} =$	2.5 × 10 ⁻⁷ mol/cm ³ (in pore water)		
Chloride Threshold Parameters	$C_{T0} =$	1.78 kg/m ³		
	$E_{T0} =$	-100 mV		
	$\beta_{CT} =$	550 mV/decade of Cl ⁻		
Polarization Parameters	E_0 (-mV SCE)	i_0 (A/cm ²)	Tafel Slope (mV)	
Iron Dissolution	-780	1.875 × 10 ⁻⁸	60	
Oxygen Reduction	160	6.25 × 10 ⁻¹⁰	160	
Steel Passive Current Density	$i_p =$	0.058 × 10 ⁻⁶ A/cm ²		
Critical Corrosion Penetration	$P_{CRIT} =$	0.01 cm		

RESULTS AND DISCUSSION

Correction Function

Representative examples of the comparative output of the cases explored in Scheme 1 (systematic parameter distributions, systematic resistivity variations) and Scheme 2 (random X_c , random C_s and combined random profile) are shown in Figure 4 and in Figure 5, respectively. At lower ages and lower levels of damage (e.g. a few %) the manifestations of early damage for PDT and PIT tended to appear at comparable times but with some variability, with one or the other taking the lead by a few years over the other. Instances where PDT took the lead at early damage levels appeared to be more evident in cases where the system parameters were subject to random variations, and less so when systematic changes with elevation dominated. As noted elsewhere the instances where PDT takes the lead may be explained as being the result of a propagation stage phenomenon and, paradoxically, a result of the delay in other activation events following the first ones.²¹ That delay enables sustained macrocell enhancement of the relatively few early active regions with consequent faster local corrosion rates for those few regions, causing their early declarations of damage. In contrast, for PIT the rate of appearance of new active regions is not decreased and thus the remaining cathodic portion of the steel assembly has to support an increasing number of anodes, with consequent less enhancement of the corrosion rate in those anodes and slower onset of the damage declarations.

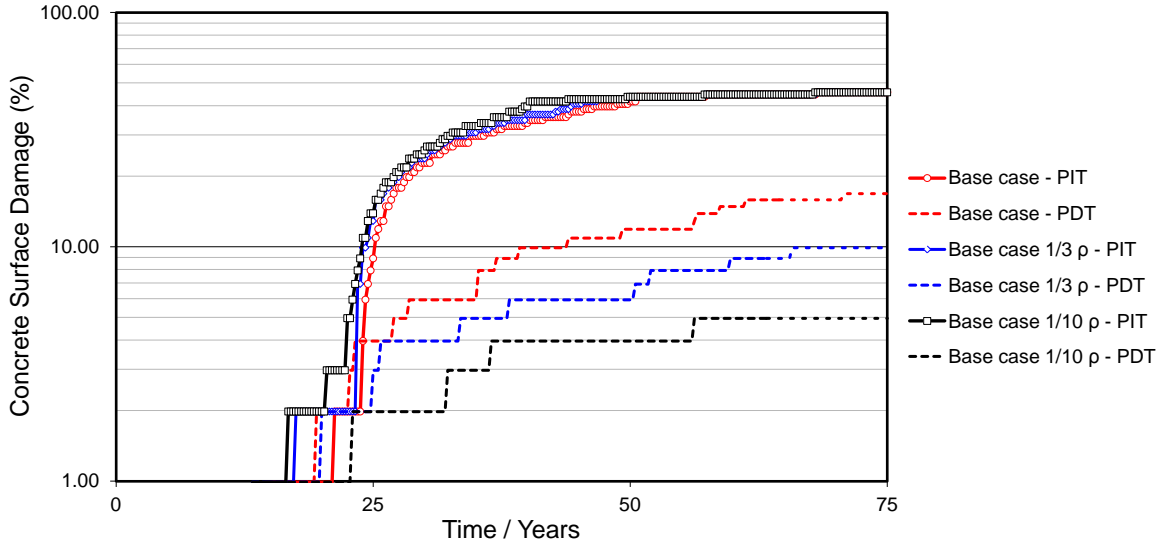


Figure 4: Example of comparative PIT-PDT output for Scheme 1 cases where resistivity at each elevation level was varied from the base case by multiplication factors of 1, 1/3 and 1/10.

The dominant trend of significantly lower amount of long term damage for PDT compared with PIT was observed in these scenarios as well as all the other variations examined. Examination of the shape and magnitude of the damage functions calculated for PDT-PIT pair combinations from the Table 1 cases showed that the long term (i.e. 75 year) ratio of PIT to PDT damage percent ranged from ~2 to ~5. For the purposes of practical implementation of this effect, a value of 3 is proposed as being representative of a *long term correction ratio* C_{LTR} . It is noted that the behavior differentiation described here as taking place in the long term is actually for an extended but intermediate time period, when chloride levels at the steel depth are substantial, but have not yet become so high as to exceed the chloride threshold at the zones of greatest potential depression. However, at very long structure ages, and if the surface chloride concentration is high enough, the amount of damage in the PDT case may eventually approach the terminal amount of damage for the comparable PIT situation. Hence, the concept of a long term ratio, and the representative value adopted for it are to be considered as working approximations subject to update and refinement in future investigations.

The parameter choices in these simulations have been conducted with values that tended to result in relatively short times to corrosion initiation, in order to reduce the need for long computational runs while still spanning a large range of total damage development. Hence, the calculations tended to emphasize the effect of propagation period-related differentiation such as the one just discussed above. That type of effect is expected to be relatively modest in the overall service life (many decades) estimate for the structures commonly designed by major transportation agencies, where highly impermeable concrete is often specified in the design phase when the environment is aggressive.²² In such concretes the values of the chloride diffusion coefficients are very small and consequently the initiation stage is the dominant period in the service life of the structure, while the propagation stage-related phenomena tend to be less important. Therefore, the differentiation between PDT and PIT cases in the early stages of damage may be considered in such cases as being of secondary importance.

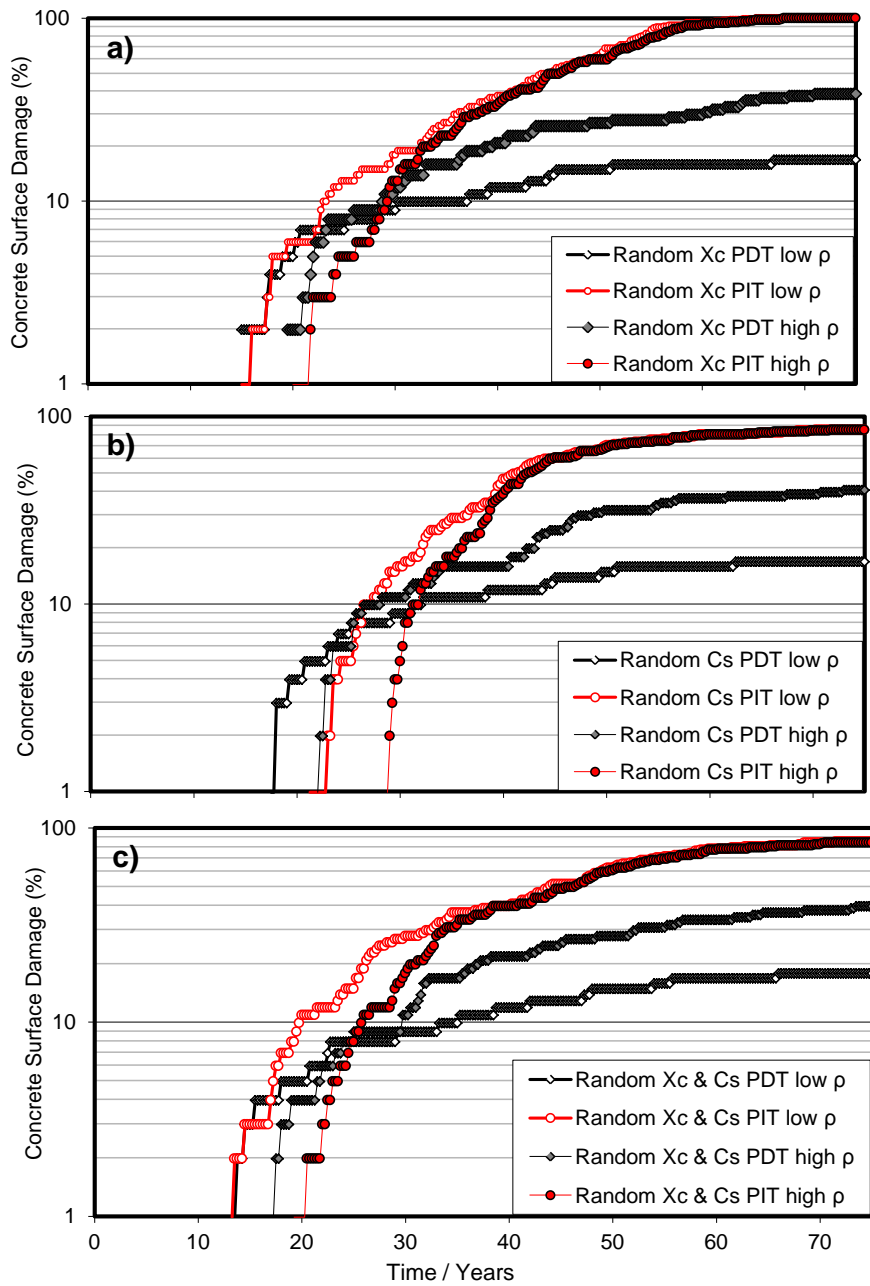


Figure 5: Example of comparative PIT-PDT for Scheme 2 cases. a) Randomly distributed X_c . b) Randomly distributed C_s . c) Combined case ²².

Based on the previous discussion and on the results of the simulations conducted, a working approximation is proposed whereby the damage projection for PDT conditions was considered to be the same as that for PIT conditions up to a *nominal crossover value* $C_{CR} = 2\%$. Further refinement of that value and of its underlying concept should be addressed by future investigations. Additionally, an adjustable provisional nominal values for the long-term correction ratio $C_{LTR} = 3$, and for the crossover damage percent $C_{CR} = 2\%$ is tentatively adopted. Then for the entire service life forecast of the

structure the corrected damage function DF is obtained from the preliminary damage function PDF by Equation (2):^{22,23}

$$DF = PDF(t) * \gamma(PDF(t)) \quad (2)$$

with the PDT Partial Factor γ defined by Equations (3) and (4):

$$\gamma = 1 \quad \text{for } PDF(t) < C_{CR} \quad (3)$$

$$\gamma = \frac{1}{1 + (C_{LTR} - 1) \cdot \frac{PDF(t) - C_{CR}}{100\% - C_{CR}}} \quad \text{for } PDF(t) \geq C_{CR} \quad (4)$$

Reflecting the above observations, at long ages when PDF approaches 100% in severe environmental exposures, γ approaches $1/C_{LTR}$. At short ages the value of γ becomes increasingly close to unity while approaching the crossover early regime. Equation (4) presupposes that for the structure (or structure portion) considered the exposure conditions are severe enough that given a sufficiently long service time, the PDF would reach nearly 100% damage. The equation also implies that the distribution of times to damage declaration is not distinctly multimodal, with some region dominating the development of damage ahead of one or more other regions. In multimodal cases Eq. (4) would have to be applied to each distinct region separately. That was indeed the case in Scheme 1, where damage on the above-water half dominated during much of time interval investigated, so the apparent terminal damage was 50% instead of 100%. For that scheme the value of C_{LTR} was calculated via the PIT-PDT damage ratio during the interval considered only. Clearly for distinctly multimodal cases application of Equation (4) without any parsing for local conditions would only serve as a rough approximation. Thus, Equation (4) represents a working compromise pending the development of more sophisticated approaches in the future.

The partial factor method introduced here was recently employed in a modeling approach developed for projecting the extent of reinforced concrete corrosion-related damage in marine bridges in subtropical service, described in detail in Ref. 22. The model incorporates a series of advanced features that include as a first stage a probabilistic treatment of the damage prediction calculations with statistical variability in C_S , X_C , and D . Additional features are type of rebar material, geometric aggravation effects from rebar presence, and corners and curvature in the concrete surface. The model has also functionality for variability in environmental aggressiveness conditions as a function of elevation above water and for location of structural components in various environments in the same bridge. Each set of similar structural and exposure regime conditions is named a *Class*, and preliminary damage functions (PDF) using the PIT assumption are calculated for each Class. The correcting γ factor introduced above is then applied as a time-dependent multiplier and an adjusted damage function (DF) is then obtained for each Class. Figure 6 illustrates the application of the concept to a Class consisting of the flat surface portion of square piles exposed to splash evaporation regimes in a marine bridge, showing the functions PDF, γ and DF for the system as function of time.²² The end result shows how this approach captures the significantly slower development of predicted damage at long structure ages when PDT is introduced in the forecast. Follow up work is in progress for the further development of this tentative approach to implementation of PDT effects on corrosion induced damage forecasting.

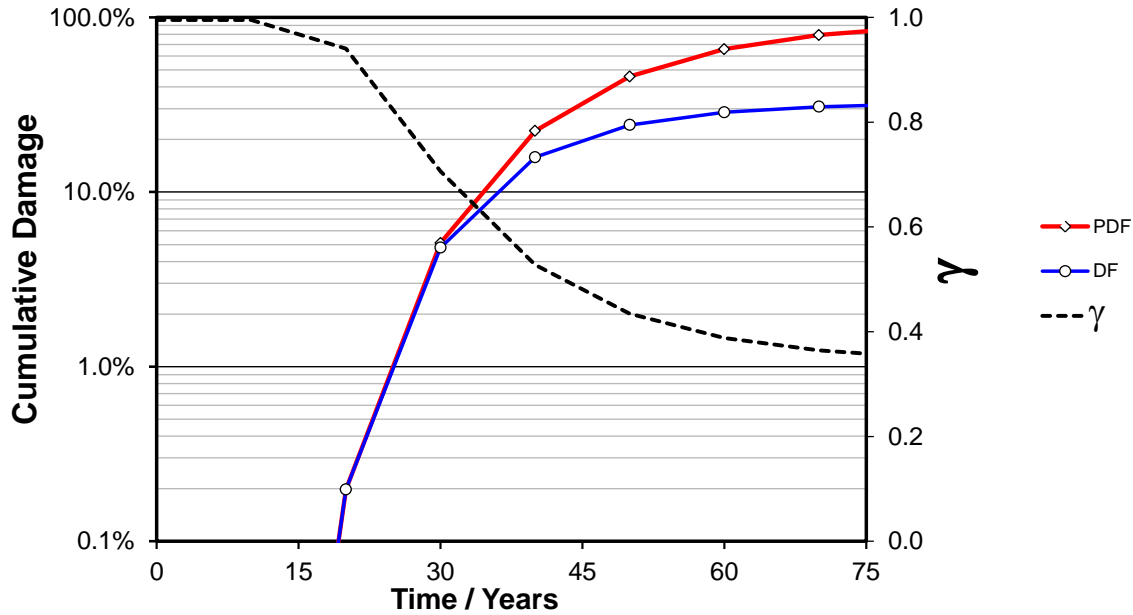


Figure 6: Example of the application of Equation (4) to long-term concrete corrosion damage projection for a marine structure²²

CONCLUSIONS

Integration of a full probabilistic corrosion forecasting approach and a Potential Dependent Threshold feature was developed and provisionally achieved via a correction function that links both modalities. The correction factor was abstracted from comparative calculations using representative marine corrosion scenarios.

The resulting forecast captures the significantly slower development of predicted damage at long structure ages when PDT is introduced. Follow up work is anticipated to refine this methodology.

ACKNOWLEDGMENT

This investigation was supported by the Florida Department of Transportation. The opinions and findings stated here are those of the authors and not necessarily those of the funding agency.

REFERENCES

1. K. Tuutti, "Corrosion of Steel in Concrete", Swedish Cement and Concrete Research Institute, Stockholm, 1982
2. A. A. Sagüés, "Modeling the Effects of Corrosion on the Lifetime of Extended Reinforced Concrete Structures", Corrosion, vol. 59, pp. 854-866, 2003.
3. Duracrete "General guidelines for durability design and redesign." The European Union-Brite Eu Ram III, Project No. BE95-1347:'Probabilistic Performance Based Durability Design of Concrete Structures', Document 15 (2000).
4. E. Bentz, "Probabilistic Modeling of Service Life for Structures Subjected to Chlorides" ACI Materials Journal, vol. 100, pp. 391-397, 2003.
5. Model Code for Service Life Design, fib Bulletin 34, ISBN: 978-2-88394-074-1, fédération internationale du béton, Lausanne, Switzerland, 2006.

6. "Life-365 Service Life Prediction Model™ and Computer Program for Predicting the Service Life and Life-Cycle Costs of Reinforced Concrete Exposed to Chlorides". (2008) Produced by the Life-365 Consortium II.
7. J. Marchand and E. Samson, "Predicting the service-life of concrete structures – Limitations of simplified models" *Cement and Concrete Composites*, vol. 31, pp. 515-521, 2009.
8. W.H. Hartt, "Corrosion Initiation Projection for Reinforced Concrete Exposed to Chlorides: Part 1—Black Bars", *Corrosion*, vol. 67, pp. 086002-1-086002-10, 2011.
9. L. Tang and A. Lindvall, "Validation of Models for Prediction of Chloride Ingress in Concrete Exposed in De-Icing Salt Road Environment", *International Journal of Structural Engineering*, vol. 4, pp. 86-99, 2013.
10. C. Andrade, "Probabilistic Treatment of the Reinforcement Corrosion" *Corrosion*, vol. 70, pp. 643-651, 2014.
11. A.A. Sagüés, A.N. Sánchez, K. Lau, and S.C. Kranc, "Service Life Forecasting for Reinforced Concrete Incorporating Potential-Dependent Chloride Threshold", *Corrosion*, vol. 70, pp. 942-957, 2014.
12. G. K. Glass and N.R. Buenfeld. "The Presentation of the Chloride Threshold Level for Corrosion of Steel in Concrete", *Corrosion Science*, 39 (5), pp. 1001-1013, 1997.
13. U. Angst, B. Elsener, C. K. Larsen, and Ø. Vennesland, "Critical chloride content in reinforced concrete — A review" *Cement and Concrete Research*, vol. 39, pp. 1122-1138, 2009.
14. C. Alonso, M. Castellote, and C. Andrade, "Chloride threshold dependence of pitting potential of reinforcements" *Electrochimica Acta*, vol. 47, pp. 3469-3481, 2002.
15. F. J. Presuel-Moreno, A. A. Sagüés, and S. C. Kranc, "Steel Activation in Concrete Following Interruption of Long-Term Cathodic Polarization", *Corrosion*, vol. 61, pp. 428-436, 2005
16. A. N. Sánchez and A. A. Sagüés, "Chloride Threshold Dependence on Potential in Reinforced Mortar". Paper No. 1728, presented at the NACE Corrosion 2012, Salt Lake City, UT. NACE International, Houston, TX., 2012.
17. A. N. Sánchez and A. A. Sagüés, "Chloride Corrosion Threshold Dependence on Steel Potential in Reinforced Concrete". Paper No. 4118, presented at the NACE Corrosion 2014, San Antonio, TX. NACE International, Houston, TX., 2014.
18. J. Bockris and A. K. N. Reddy, Volume 1: *Modern Electrochemistry: Ionics*, 2nd ed. Plenum Press, New York, 1998.
19. P. Pedferri, "Cathodic Protection and Cathodic Prevention", *Construction and Building Materials*, vol. 10, pp. 391-402, 1996.
20. F. J. Presuel-Moreno, S. C. Kranc, and A. A. Sagüés, "Cathodic Prevention Distribution in Partially Submerged Reinforced Concrete", *Corrosion*, vol. 61, pp. 548-558, 2005.
21. A. N. Sánchez and A. A. Sagüés, "Probabilistic Corrosion Forecasting of Steel in Concrete with Potential-dependent Chloride Threshold" pp. 408-415, *Proceedings of the 1st International Conference on Ageing of Materials & Structures*. Editors: K. van Breugel and E.A.B Koenders. Delft University of Technology. Delft, The Netherlands, 2014
22. A. N. Sánchez and A. A. Sagüés, "Modeling Reinforced Concrete Durability". Final Report Contract No. BDK84 977-09" Florida Department of Transportation Research Center, Tallahassee, FL., 2014.
23. A.N. Sánchez and A.A. Sagüés, "Some Open Issues in Forecasting Corrosion Risk of Steel in Concrete", *Corrosion*, vol. 70, pp. 1148-1156, 2014.